Effect of receiver movement on signal detection in an ultrasonic LPS

Fernando J. Álvarez, Teodoro Aguilera, José A. Paredes, Jorge Morera, J. Álvaro Fernández
Department of Electrical Engineering, Electronics and Automatic
University of Extremadura. 06006 Badajoz, Spain
Email: fafranco@unex.es

***Abstract*—This work analyses the effect of the receiver movement on the pulse compression of the signals emitted by the beacons of an Ultrasonic Local Positioning System (ULPS). This analysis is first carried out by using a system model in order to obtain a set of results that are then experimentally validated with the help of an electric slider. The signals emitted by the ultrasonic beacons are encoded with Kasami sequences of four different lengths (15, 63, 255 and 1024 bits), and radial speeds of up to 2 m/s have been considered in the experimentation. The results derived from this study should be of interest to anyone performing matched filtering of ultrasonic signals with a moving emitter/receiver.**

***Index Terms*—LPS, Doppler shift, Pulse compression, Kasami sequences**

I. Introduction

Local Positioning Systems (LPS), intended to locate people and/or objects in indoor environments, constitute one of the core elements of the so called Intelligent Environments (IE). In the last years we have witnessed a growing interest in the development of this type of systems, with the appearance of proposals based on different technologies including ultrasonic [1], magnetic [2], optic [3] and radiofrequency [4]. Among them, ultrasound represents a classic solution whose popularity comes from its low cost and high reliability.

Yet during the first years of the former decade, some systems were proposed that achieved centimetric precision through the emission of ultrasonic pulses, both centralized, where the object to be located acts as the emitter [1], and localized, where this object is in charge of computing its own position using the signals received from different beacons [5]. Shortly after, signal coding was incorporated into these systems, choosing for this purpose families of binary codes with good correlation properties. This improvement brought important advantages: simultaneous emission, higher precision, larger robustness to noise and the capability to introduce privacy in the location process. Since one of the first encoding proposals carried out by Hazas and Ward with Gold sequences [6], several works have arisen in the field of ULPS that employ more and more complex encoding schemes, with the emission of Kasami sequences [7] and, more recently, Loosely Synchronous (LS) codes [8].

Many authors have already pointed out the problems that the receiver movement could cause on the detection of ultrasonic encoded signals, since the Doppler effect undergone by these signals could make them completely unrecognizable to the matched filter installed in the receiver [9], [10]. In a recent work, the authors have presented a complete software model for a ULPS that can be used to simulate this effect [11], and it was shown that radial speeds as low as 1.5 m/s could drastically deteriorate the autocorrelation properties of the signals emitted by this system: 255-bit Kasami sequences with BPSK modulation at 50 kHz.

In this paper, a detailed analysis of this phenomenon is presented by quantifying the increment of the auto- and cross-correlation bound of four different families of Kasami codes with increasing speed of the receiver. The analysis is first performed with a high versatility simulator, that allows the user to choose among different families of codes and modulation schemes, as well as to model the effect of various phenomena that characterize the propagation of ultrasonic signals in the air: geometrical spreading, atmospheric absorption and the filtering associated with the transducers. Next, the results obtained with this simulator for a particular family of codes and modulation scheme are experimentally validated making use of an electric slider with which the speed of the ultrasonic emitter/receiver can be accurately controlled. The main conclusions of this work are finally outlined in the last Section.

II. Simulated Model

As stated before, the LPS system under analysis is based on the emission of Kasami sequences, that belong to the well known family of pseudorandom codes [12]. A new Kasami sequence k can be generated from a maximal sequence and the decimated and concatenated version of this sequence by performing the module-2 sum of the former with any delayed version of the latter, i.e.,

$$k = m_1 \oplus D^l m_2 \qquad \text{with } l < L \tag{1}$$

where m_1 is a maximal sequence of length $L = 2^{N-1}$ with N even, m_2 is the sequence obtained from the decimation of m_1 with a decimation factor of $q = 2^{N/2}+1$ and the concatenation of the result q times, $\oplus$ represents the module-2 sum and $D^l m_2$ is the sequence obtained by cyclically shifting l positions the m_2 sequence.

In order to adapt the spectral features of the emission to the frequency response of the ultrasonic emitter, these codes are binary phase modulated (BPSK). This modulation scheme has been widely used to transmit binary codes in matched filtering-based sonar systems. Every bit in the code $k[n]$ is modulated

with one or more carrier cycles whose phase, 0 or π, is given by the bit value to obtain the modulated pattern as:

$$p[n] = \sum_{i=0}^{L-1} k[i] \cdot \mathrm{m}\left[n - i \cdot N_c \cdot M\right] \tag{2}$$

where L is the code length, $\mathrm{m}[n]$ is the modulation symbol formed by N_c carrier cycles, and M represents the number of samples per period (ratio between the sampling and the carrier frequencies). A common measure for the performance of a family of K modulated codes is given by the autocorrelation (AC) and crosscorrelation (CC) bounds, defined as:

$$\theta_{AC} = \max\left\{\frac{\phi_{s_i p_i}[k]\,\forall k \notin [-M, M]}{\max \phi_{s_i p_i}} \quad \forall i \in \{1, \ldots, K\}\right\} \tag{3a}$$

$$\theta_{CC} = \max\left\{\frac{\phi_{s_i p_j}[k]\,\forall k}{\max \phi_{s_i p_i}} \quad \forall i, j \in \{1, \ldots, K\}, \quad i \neq j\right\} \tag{3b}$$

where $\phi_{sp}[k]$ is the aperiodic correlation function between the received signal s and the stored pattern p, and M is again the number of samples in a carrier period. The first bound will give a measure of the difficulty to detect a code received at a certain speed, whereas the second bound will show how the cross-correlation properties of the family are deteriorated as a consequence of this movement. Depending on the application, the upper threshold for these magnitudes are typically in the range 0.3 - 0.5.

The effect of the receiver movement can be easily simulated by assuming a virtual sampling frequency for the emitted signal:

$$f_s' = f_s\left[1 - \frac{\vec{v}_e}{\mathrm{c}}\frac{\vec{r}_e - \vec{r}_r}{|\vec{r}_e - \vec{r}_r|}\right] \tag{4}$$

where f_s is the actual sampling frequency, $\mathrm{c} \simeq 343$ m/s is the sound speed in air at a temperature of 20°C and pressure of 1 atm, $\vec{r}_e$ is the emitter position vector, $\vec{r}_r$ is the receiver position vector, and $\vec{v}_r$ is the receiver velocity vector. From this frequency, the signal acquired by the receiver at the actual sampling frequency is obtained by cubic spline interpolation [13].

Fig. 1 shows the results obtained for the autocorrelation bound when applying this model to four Kasami sequences with different lengths of 15, 63, 255 and 1023 bits. All these codes are BPSK modulated with a symbol of one carrier cycle and assuming a sampling frequency ten times greater than the carrier frequency. This figure shows the θ_{AC} variations for a receiver radial velocity ranging from -10 m/s to 10 m/s. This figure makes evident a well-known result in radar theory: the shorter the code length the larger its robustness to Doppler shift. As can be seen, for a detection threshold of $\theta_{AC} = 0.4$, the maximum admissible radial velocities would be (in module) 9.37, 3.76, 1.16 and 0.35 m/s when using Kasami codes of lengths 15, 63, 255 and 1023 bits respectively.

As stated in the Introduction, one of the main advantages of encoding the ultrasonic signals of a LPS, is the capability to perform the simultaneous emission of all the beacons

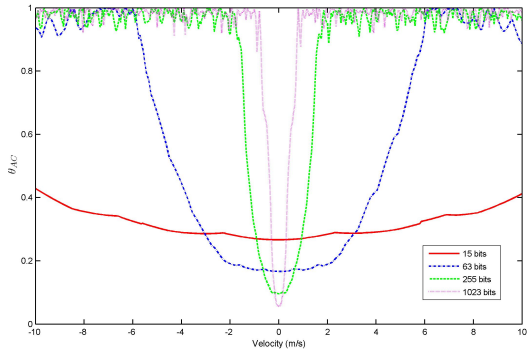

Fig. 1. Autocorrelation bound of the family (15, 63, 255 and 1023 bits).

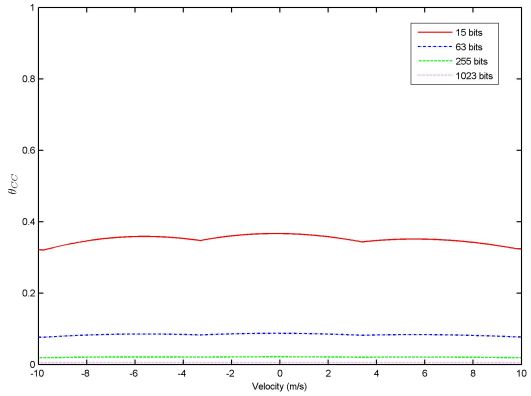

Fig. 2. Crosscorrelation bound of the family (15, 63, 255 and 1023 bits)

whose signals will be distinguished by the receiver despite their possible overlapping. For this reason, it is important to analyze the effect of the receiver movement not only in the autocorrelation of the emitted codes, but also in the cross-correlations between all the codes in the family. In this work, we have supposed that our LPS is composed of four beacons performing the simultaneous emission of Kasami codes with good correlation properties. Fig. 2 shows the results obtained for the crosscorrelation bound θ_{CC} as a function of the receiver velocity, for all lengths under consideration. This figure shows that the receiver movement does not significatively worsen the crosscorrelation properties of these codes with respect to the values obtained with a stationary receiver.

III. Experimental Analysis

This section presents the experimental analysis carried out to validate the simulated results obtained in the previous section. A picture of the experimental equipment employed in this analysis is shown in Fig. 3. This equipment is composed of:

1) Computer: from where a software application controls the emission, the movement of the platform supporting the emitter, and the acquisition parameters. The received data are stored in a text file for their latter processing.
2) Electric slider: two meters long conveyor belt where the ultrasonic transducer is fixed. A small platform has been built to separate the emitter from the base and

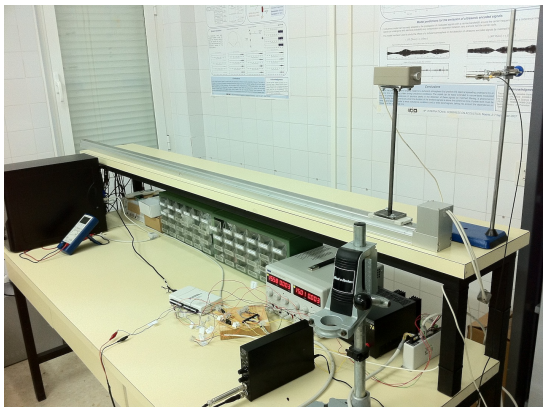

Fig. 3. Experimental setup.

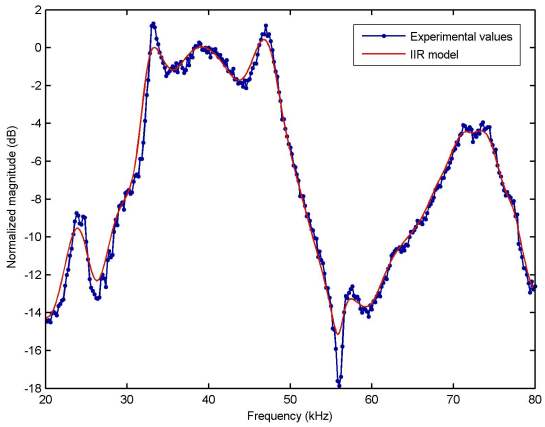

Fig. 4. Emitter frequency response: experimental values (blue dotted) and IIR filter model (red solid).

avoid undesired echoes. This slider is capable to reach a maximum speed of 2 m/s, with maximum acceleration values of ± 3 m/s^2, thus providing an analysis window of about 800 ms of constant velocity.

3) Two DC sources: one providing 24 V and 7 A for the electric slider, and the second providing 24 V and 3 A for the controller.
4) NI USB-6212 data acquisition card, to transmit the modulated code to the emitter and acquire the signal received by the microphone at a sampling frequency of 400 kS/s.
5) Prowave 400WB160 ceramic ultrasonic transducer, with a central operation frequency of 40.0$\pm$1.0 kHz, a nominal bandwidth of 10 kHz at -6 dB, and a sound pressure level (SPL) of 105 dB min ref. to 20 μPa at 30 cm. A driver module has been specifically designed for this transducer, based in a TL082 operational amplifier in inverting configuration, providing a gain of -3 V/V.
6) G.R.A.S. 40BE free-field prepolarized ultrasonic microphone, with a sensitivity of 4 mV/Pa, a dynamic range of 3-166 dB re. to 20 μPa, and a flat frequency response in the range 4 Hz - 100 kHz.
7) G.R.A.S. 12AK power module, that provides a signal amplification of 40 dB in the range of frequencies of interest and performs a high-pass filtering with a cutoff frequency of 20 Hz.

A. Transducer response and atmospheric absorption modeling

Prior to obtaining experimental data with the equipment described above, two phenomena characterizing this particular experimentation must be included in the model employed in Section II, since they could have a strong influence on the simulated results. These phenomena are:

1) The frequency response of the ultrasonic transducer, with a nominal bandwidth of 10 kHz at -6 dB according to the manufacturer.
2) Atmospheric absorption of ultrasound in air at the laboratory temperature and humidity conditions. This absorption coefficient is strongly dependent on frequency.

To model the first phenomenon, an accurate experimental analysis of the frequency response of the the emitter (driver + transducer) has been carried out in the range 20 kHz - 80 kHz, obtaining the results shown in Fig. 4 (blue dotted line). This response has been modelled with a 50 order IIR filter whose frequency response is also represented in Fig. 4 with a red solid line.

With respect to the atmospheric absorption of ultrasound in air, it has been modeled as dictated by the ISO 9613-1 (1993) standard [14]. To emulate the laboratory conditions, a temperature of 20^{o}C, a relative humidity of 60% and an atmospheric pressure of 1 atm have been assumed. Also, an average separation distance of 1 m between the emitter and the receiver has been considered. In all cases, we have observed that the variations taking this phenomenon into account are negligible. A new set of simulations have proved that the frequency dependence of the absorption coefficient would start distorting the received signal for a emitter-receiver distance of about 20 meters, a distance that is unlikely to be usable in practice, given the reduced SPL of our emitter.

B. Results

The experimental analysis has been carried out by increasing the emitter velocity from 0 to 2 m/s in steps of 0.1 m/s for all code lengths under consideration. The values obtained for the θ_{AC} are represented in Figs. 5 and 6 for the lengths of 63 and 255 bits respectively, together with the ideal simulation and the simulation that takes into account the frequency response of the emitter. The experimental values have been fitted to a second order polynomial in the form $\theta_{AC}(v) = \mathrm{A} + \mathrm{B}\ v + \mathrm{C}\ v^2$, which is also represented in these figures as a solid line. The values obtained for these coefficients in all cases are shown in Table I.

Finally, Fig. 7 shows the values of θ_{CC} obtained for the lengths of 63 and 255 bits, together with the predictions of the simulation that models the frequency response of the emitter. This figure corroborates the results already shown in Fig. 2, i. e., the Doppler effect does not significatively deteriorate the values of the crosscorrelation bound.

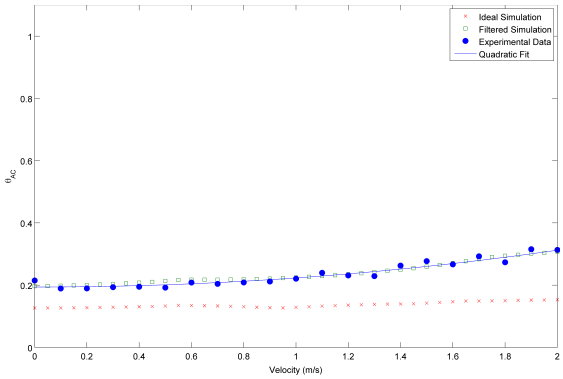

Fig. 5. Experimental values of autocorrelation bound for 63 bits.

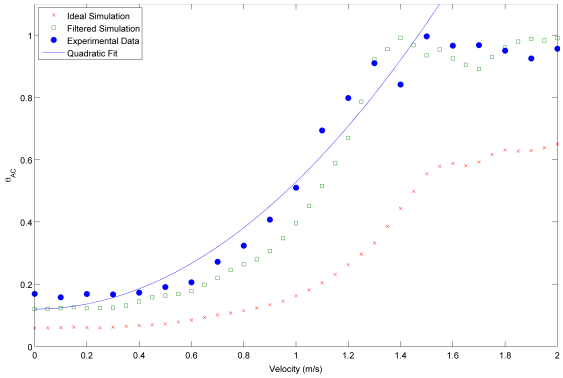

Fig. 6. Experimental values of autocorrelation bound for 255 bits.

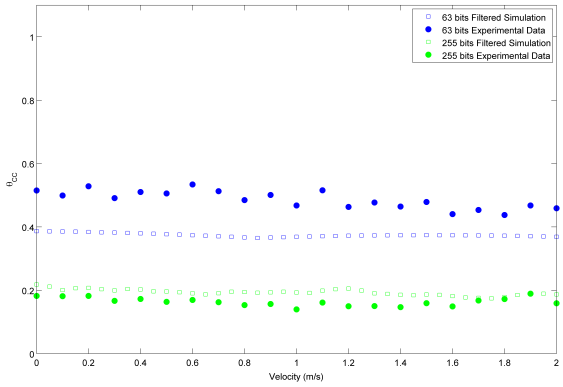

Fig. 7. Experimental values of crosscorrelation bound for the families of 63 and 255 bits.

TABLE I
FITNESS COEFFICIENTS FOR

$$\theta_{AC}(v) = \mathrm{A} + \mathrm{B}\, v + \mathrm{C}\, v^2$$

	A	B	C
15 bits	0.2817	0.0011	0.0007
63 bits	0.1941	−0.0007	0.0299
255 bits	0.1200	0	0.4083
1023 bits	0.1796	0	2.0547

IV. Conclusions

This work has presented a detailed study of the influence that the receiver velocity can have on the matched filtering of the signals emitted by a particular ultrasonic LPS. Four BPSK modulated Kasami families with different lengths have been considered in this study, establishing for each one of them the range of admissible receiver velocities in terms of the autocorrelation bound of the corresponding family. These results have been experimentally validated with the help of an electric slider, and these experimental data have been fitted to a second order polynomial that can be used to easily determine the worsening of the bound as a function of the receiver velocity.

Acknowledgements

This work has been partially supported by the Spanish Ministry of Science and Innovation, through the project LEMUR-UEx (ref. TIN2009-14114-C04-04), and the Regional Government of Extremadura, through the European Regional Development Funds (FEDER)

References

[1] M. Addlesee, R. Curwen, S. Hodges, J. Newman, P. Steggles, A. Ward and A. Hopper, *Implementing a Sentient Computing System*, IEEE Computer, Vol. 34 (8), pp. 50–56, Aug. 2001

[2] J. Blankenbach and A. Norrdine *Position Estimation Using Artificial Generated Magnetic Fields*, 2010 International Conference on Indoor Positioning and Indoor Navigation (IPIN), Zürich, Switzerland, Sept. 2010.

[3] S. Tilch and R. Mautz, *Current investigations at the ETH Zurich in optical indoor positioning*, 7th Workshop on Positioning Navigation and Communication, pp. 174-178, Dresden, Germany, March 2010.

[4] K. Arshak and F. Adepoju, *A model for estimating the real-time positions of a moving object in wireless telemetry applications using RF sensors*, in Proc. of the 2007 IEEE Sensors Applications Symposium, San Diego, USA, Feb. 2007.

[5] C. Randell and H. Muller, *Low Cost Indoor Positioning System*, Proc. of the 3rd International Conference on Ubiquitous Computing, pp. 42–48, Atlanta, USA, Sept. 2001.

[6] M. Hazas and A. Ward, *A High Performance Privacy-Oriented Location System*, Proc. of the 1st IEEE International Conference on Pervasive Computing and Communications (PerCom 2003), pp. 216–223, Dallas, USA, March 2003.

[7] J. Ureña, A. Hernández, J. M. Villadangos, M. Mazo, J. C. García, J. J. García, F. J. Álvarez, C. de Marziani, M. C. Pérez, J. A. Jiménez, A. Jiménez and F. Seco, *Advanced Sensorial System for an Acoustic LPS*, Microprocessors and Microsystems, Vol. 31 (6), pp. 393–401, 2007.

[8] M. C. Pérez, J. Ureña, A. Hernández, A. Jiménez, D. Ruíz, C. de Marziani and F. J. Álvarez, *Efficient hardware implementation for detecting CSS-based Loosely Synchronous codes in a Local Positioning System*, 2009 IEEE Conference on Emerging Technologies and Factory Automation, Mallorca, Spain, Sept. 2009.

[9] S. Holm, *Hybrid Ultrasound-RFID Indoor Positioning: Combining the Best of Both Worlds*, 2009 IEEE International Conference on RFID, pp. 155-162, Orlando (FL), USA, April 2009.

[10] M. Alloulah and M. Hazas, *An efficient CDMA core for indoor acoustic position sensing*, 2010 International Conference on Indoor Positioning and Indoor Navigation (IPIN), Zürich, Switzerland, Sept. 2010.

[11] Fernando J. Álvarez, Teodoro Aguilera, Juan A. Fernández, José A. Moreno and Antonio Gordillo, *Analysis of the Performance of an Ultrasonic Local Positioning System based on the emission of Kasami codes*, 2010 International Conference on Indoor Positioning and Indoor Navigation (IPIN) Zürich, Switzerland, Sept. 2010.

[12] T. Kasami, *Weigh distribution formula for some class of cyclic codes*, Technical Report R-285, Coordinated Science Lab. University of Illy-nois, 1966.

[13] C. F. Gerald and P. O. Wheatley, *Applied Numerical Analysis*, Addison-Wesley, 1994.

[14] ISO/TC 43 Technical Comittee, Acoustics, Sub-Comittee SC1, Noise, *Attenuation of sound during propagation outdoors. Part 1: Calculation of the absortion of sound by the atmosphere*, Technical Report ISO 9613-1:1993(E), International Organization fot Standarization, 1993.